Nanowiring

Flexible Nanowiring of Metal on Nonplanar Substrates by Femtosecond-Laser-Induced Electroless Plating**

Bin-Bin Xu, Hong Xia, Li-Gang Niu, Yong-Lai Zhang, Kai Sun, Qi-Dai Chen, Ying Xu, Zhi-Qiu Lv, Zhi-Hong Li, Hiroaki Misawa, and Hong-Bo Sun**

In recent years, metal nanowiring for circuitry and electronic interconnection has attracted much attention due to the growing requirements of highly integrated microcircuits, and is of benefit to the miniaturization of device features.[1] Generally, ultraviolet photolithography, which was considered a typical processing route for metal wiring, has already greatly contributed to integrated circuits.[2] However, the lithographic route shows strong demands on the surface flatness of each layer in the multilevel chip architectures. To meet the processing nature of lithography, a global planarization of interlayer metals by chemical–mechanical polishing is therefore needed to reduce the interval between the metal layer and the photomask, and to guarantee exposure resolution when wires reach the sub-300 nm scale. Two-photon absorption (TPA) has also been tried for the fabrication of metal microstructures by using suitable salt solutions as the metal source and photosensitive molecules as the photoinitiator.[3–5] However, these studies aimed at refined planar periodic gratings or dot arrays[6] for plasmonic wave coupling or three-dimensional (3D) mold making, which more or less ignore the conductivity of these precise metal structures. For example, by using surfactants as particle-growth inhibitor, delicate 3D structures with a smooth surface were achieved,[7] whereas the conductivity of these metal microstructures was significantly debased due to the residual organic components.

To the best of our knowledge, both the photolithography and TPA micro/nanoprocessing conducted so far have focused on fabrication on flat substrates.[8–10] These methods cannot meet the increasing demands of circuitry and electronic connections on nonplanar substrates in microelectromechanical systems (MEMS),[1] lab on a chip (LoC),[11] and other intelligent microsystems. Taking LoC as an example, if an appropriate microheater could be embedded on the immediate base inside a microfluidic channel instead of sitting several hundreds of micrometers apart on the rear of the substrate, as is usually done with Peltier thermoelectric elements,[12] integrated resistive heaters,[13–17] and Joule heating of ionic liquids,[18] then local temperature regulation of fluids with higher precision, quicker response, and smarter switching at the exact point of care may be realized due to the effectively reduced thermal inertia. Such a capability is particularly desired for temperature regulation of miniaturized LoC systems that involve repeated thermal cycling, such as DNA amplification by the polymerase chain reaction (PCR), which comprises three sequential steps of denaturation (95 °C), annealing (55 °C), and extension (72 °C).[12] Nevertheless, convenient introduction of a local heating circuit inside a ready channel is almost inaccessible for lithography and other currently available micro/nanofabrication methods. Therefore, there is an urgent need for flexible micro/nanoprocessing technologies for metal nanowiring on nonplanar substrates or existing device structures.

Herein, we demonstrate the flexible nanowiring of metal on nonplanar substrates by femtosecond-laser-induced electroless plating. The fundamental concept consists of immersing the surface where the metal circuitry or electronic interconnection is to be made into a metal-salt solution, and then tightly focusing a near-infrared femtosecond-laser beam[19,20] onto the site to form a wire. Because of the negligible linear absorption of the solution at the laser wavelength and the fractional reflection at the air/liquid interface, the beam penetrates deeply into the solution with very small power loss, while it triggers photoreductive reactions of the metal ion via multiphoton absorption (MPA) at the focal spot. By scanning the laser focus along a preprogrammed trace following the top surfaces, either flat or nonplanar, the desired metal nanowiring is achieved.

[*] Prof. H.-B. Sun, B.-B. Xu, Dr. H. Xia, L.-G. Niu, Dr. Y.-L. Zhang
Dr. Q.-D. Chen, Dr. Y. Xu
State Key Laboratory on Integrated Optoelectronics
College of Electronic Science and Engineering
Jilin University
2699 Qianjin Street, Changchun 130012 (China)
E-mail: hbsun@jlu.edu.cn; chenqd@jlu.edu.cn
Prof. H.-B. Sun
College of Physics, Jilin University
119 Jiefang Road, Changchun 130023 (China)
Z.-Q. Lv, Prof. Z.-H. Li
Institute of Microelectronics
Peking University
Beijing 100871 (China)
Dr. K. Sun, Prof. H. Misawa
Research Institute of Electronic Science
Hokkaido University
Kita Ku, Sapporo, Hokkaido 0010021 (Japan)

[**] We would like to acknowledge the financial support from the NSFC under grants 60978048, 90923037, and 60977025.

Supporting Information is available on the WWW under http://www.small-journal.com or from the author.

DOI: 10.1002/smll.201000511

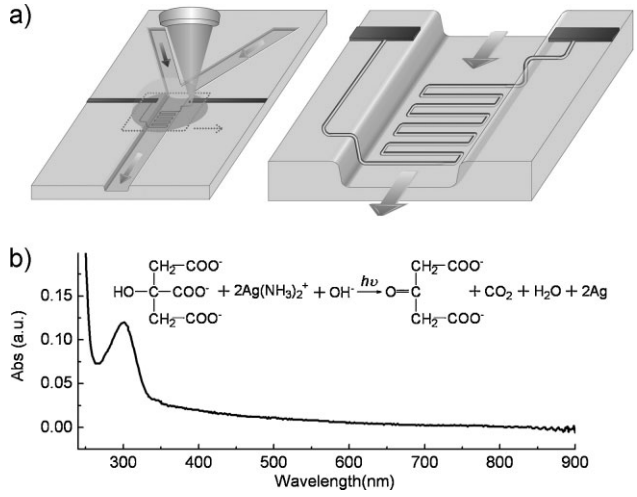

Figure 1. a) Scheme for femtosecond-laser-induced silver nanowiring in a microfluidic channel to form a microheater. b) Absorption spectrum of the silver precursor; inset: the proposed reaction equation.

As shown in Figure 1a, a ''Y-shaped'' microchannel was chosen as a representative nonplanar substrate for silver nanowiring. The purpose of this embellishment is to form a metallic microheater for highly localized temperature regulation. In the laser processing, the 790 nm femtosecond-laser pulses, with a width of 120 fs, were tightly focused on the microchannel between two precoated Au–Ge–Ni electrodes by a high-numerical-aperture (NA = 1.35, 100 ×) oil-immersion objective lens. The laser power was controlled by a gradual neutral density filter. The focal spot was scanned laterally by steering a two-galvanomirror set, and moved vertically along the optical axis by a piezo stage,[21–24] both with motion accuracy better than 1 nm. In this work, a transparent silver precursor prepared from silver nitrate, ammonia, and trisodium citrate was used as the metal source (see the Experimental Section for details). Figure 1b shows its optical absorption spectrum. It could be clearly identified that there is only one absorption band peaking at 302 nm, attributable to the silver ion. The absence of absorption at ≈790 nm (laser wavelength) indicates that the photoreduction of the silver ion is a MPA process, most probably TPA, which is of benefit to both the deep transmission of the laser beam and high-precision pinpoint writing. The inset of Figure 1b shows the proposed reaction equation. Here, trisodium citrate was chosen as a photoreducing agent[22] on account of its weak reductive ability that would provide sufficient stability for laser processing. The as-synthesized silver precursor is stable for as long as one month in the dark at room temperature (Supporting Information, Figure S1). While under femtosecond-laser irradiation, reduction occurs immediately due to the TPA process. After reduction, the citrate was proposed to be transformed to acetone-1,3-dicarboxylate according to previous reports.[24] During the formation of silver microstructures, citrate and its reduction product also act as inhibitors for the growth of silver particles,[25–28] thus giving rise to a smooth surface of as-formed microwires.

For optimizing the experimental conditions, we carefully evaluated the dependence of fabrication resolution on the laser power. As shown in Figure 2a, a series of silver nanowires was patterned on a glass slide. Their width could be adjusted simply through control of the laser power (Figure 2b). The thinnest silver nanowire patterned by the laser at 1.2 mW was only 125 nm, just a sixth of the fabrication wavelength and far beyond the diffraction limit of 790 nm laser focusing. This resulted from the combined effect of nonlinear light–matter interactions, that is, the square dependence of the absorption rate on the laser intensity and the threshold response of the metal-salt solution to the light excitation, similar to the case of photopolymerization.[29] In our case, the smallest line width was 125 nm; a further decrease of laser power (below 1.2 mW) would result in a discontinuous silver wire. In addition, the surfaces of these silver nanowires were smooth and no obvious bulky silver particles were formed all over the nanowires, which indicates that our silver precursor is very tractable for laser-induced electroless plating. In fact, any desired microstructures could be directly written on the substrate according to preprogrammed patterns. As shown in Figure 2c, a double winding was successfully produced for microheater use. For some uneven substrates, such as the bottom of a microchannel, the patterning

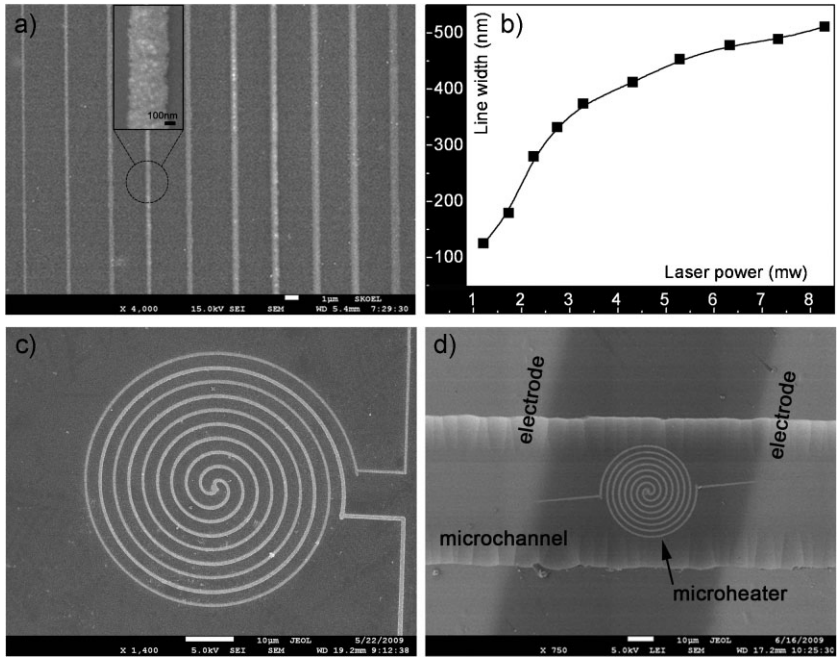

Figure 2. a) Scanning electron microscopy (SEM) image of silver nanowires patterned with a laser at different powers. Inset: magnified SEM image of a silver wire. b) Dependence of silver line width on the power of the femtosecond laser. c) SEM image of a patterned silver microcircuit on a flat substrate. d) SEM image of a patterned microheater inside a microchannel (80 μm in width and 20 μm in depth). These silver micropatterns were fabricated at a laser power of 5 mW and exposure time of 2000 μs.

of a similar silver microheater is also feasible. As exhibited in Figure 2d, a refined silver winding is successfully created between two precoated electrodes at the bottom of the microchannel (20 μm in depth and 80 μm in width). The microheater is constituted by a series of silver circles (about seven loops) only 40 μm in diameter. In addition, the silver/glass adhesion was quite robust, and almost no degradation was found on the silver circuits even after ultrasonic washing (Supporting Information, Figure S2). Therefore, it is reasonable to believe that such a microheater would show excellent performance for small-region temperature regulation in microfluidic reactions.

One of the greatest advantages of femtosecond-laser micro/nanoprocessing is its flexibility for integration. Through careful control of the laser spot, various 3D structures with nanometer spatial resolution could be fabricated on any substrate. Undoubtedly, the flexible nanowiring of silver was not limited to a rough two-dimensional surface. In this work, the powerful femtosecond-laser-induced silver electroless plating method was also applied to substrates with 3D circuitry and interconnections. As shown in Figure 3a, a hemisphere with a radius of 20 μm was firstly prepared through TPA-induced photopolymerization of SU-8 (see the Experimental Section for details), and then the silver microheater (Figure 2d) was patterned on this hemisphere. Notably, the silver microwire was well connected around this curved surface. Figure 3c gives another example: five frustums of pyramids (bevel slope: 2; height: 4 μm) were also fabricated beforehand on the substrate for silver nanowiring. As exhibited in the SEM images (Figure 3c,d), a single silver wire circle that passed over the frustums of the pyramids was created. Clearly, when viewed from the top, the patterned silver wire is well formed on the 3D structured substrate. The magnified SEM image shows that the silver microwire has a good continuity even at the corners.

Despite the well-defined microstructures, the final purpose of the metal nanowiring is to form circuitry and electronic interconnections that have strong demands for conductivity, for example as a heating circuit. To obtain refined microstructures with a smooth surface, as reported previously,[7] organic molecules such as surfactants are widely used as particle-growth inhibitors.[25,30–33] Unfortunately, the residual surfactant molecules decrease the conductivity significantly. In our experiment, the small trisodium citrate molecules with good solubility tended to diffuse into the solution without residue when the silver microstructure was formed. As shown in Figure 4, the conductivity of the silver microwire was carefully characterized. Two Au–Ge–Ni electrodes were coated on a glass substrate beforehand by evaporation technology. Then two silver wires were directly written between the two electrodes in parallel (Figure 4a). The current–voltage curve of the two parallel, connected silver wires gives a linear dependence, thus indicating good ohmic contact (Figure 4b). The atomic force microscopy (AFM) image (Figure 4c) shows that the surface of the silver nanowire is very smooth. It could be clearly identified from the height profile (Figure 4d) that the silver nanowire is about 80 nm in height. According to Ohm's law, the resistivity of our femtosecond-laser-reduced silver is estimated to be $\approx 1.7 \times 10^{-7}\,\Omega$m, only ten times larger than that of bulk silver ($1.6 \times 10^{-8}\,\Omega$m), which might be due to slight oxidation and the existence of the particle–particle intervals on the surface.

To demonstrate the application of this novel metal nanowiring, a simple microheater was prepared on the bottom of a "Y-shaped" microchannel. Then a polydimethylsiloxane (PDMS) slab was placed on the microfluidic chip to form a sealed channel. For clear observation, methylene blue trihydrate (MB; 0.1 mol L^{-1}) was injected into the microchannel (Figure 5a). Subsequently, a voltage of 1 V was

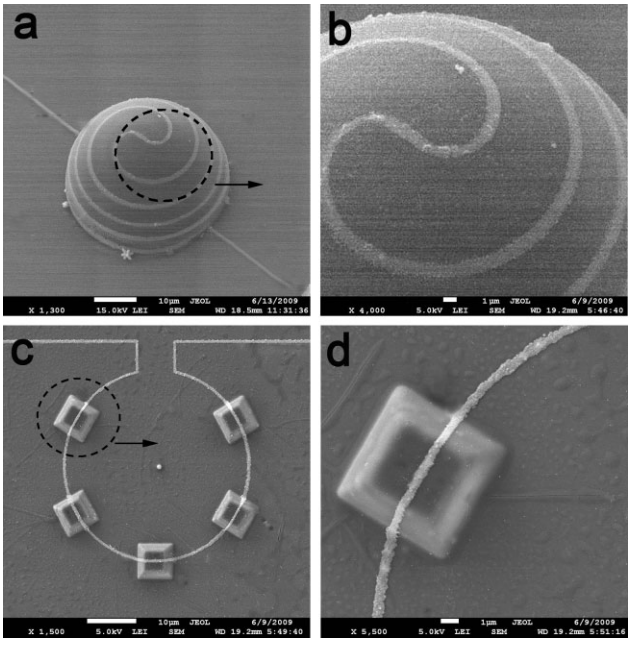

Figure 3. SEM images of silver micropatterns fabricated on substrates with 3D microstructures. a,b) Silver microwinding on a hemisphere; c,d) single silver microwire cycle on the frustum of a pyramid. These silver micropatterns were fabricated at a laser power of 7 mW and exposure time of 3000 μs.

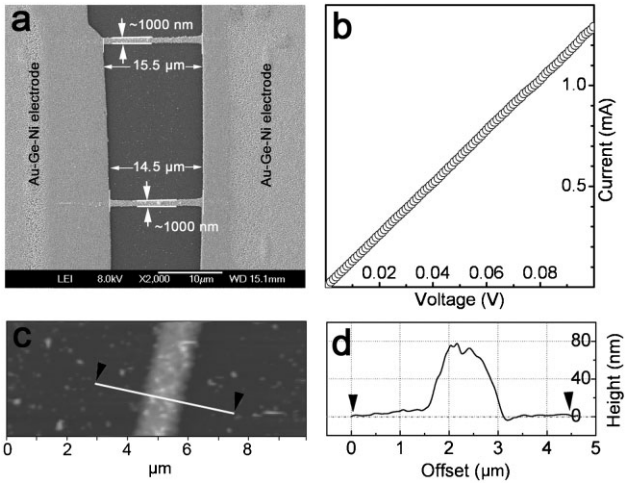

Figure 4. Resistivity characterization of patterned silver microwires. a) SEM image of silver microwires between two Au–Ge–Ni electrodes. b) Current–voltage curve of the two silver microwires. c) AFM image of the silver microwire. d) Height profile of the silver microwire.

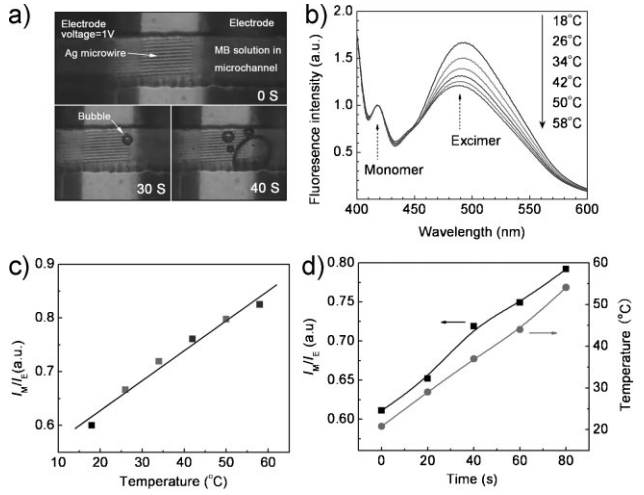

Figure 5. Heating test of a microheater fabricated inside a microchannel. a) Optical micrographs of the heating process. b) PL spectra of PS-Na at different temperatures. c) Intensity ratio of monomer to excimer versus temperature. d) Intensity ratio of monomer to excimer and temperature versus heating time.

supplied to this microheater. After about 30 s, a bubble began to emerge in the surrounding solution. Then the bubble began to grow and the bubbles increased in number. This phenomenon indicates that our microheater efficiently calorified the local liquid (see video in the Supporting Information). To quantitatively calibrate the local temperature inside the channel, 1-pyrenesulfonic acid sodium salt (PS-Na; Supporting Information, Figure S3)[33,34] was charged into the channel and the photoluminescence (PL) spectrum was monitored. As shown in Figure 5b, the peak intensities of the monomer (415 nm) and excimer (485 nm) of PS-Na have a sensitive response at ambient temperature. With an increase of temperature, the peak intensity of the monomers increased, while that of the excimers decreased. For precise detection, the excitation wavelength was fixed at 380 nm due to the best linear dependence of the peak intensity ratio (I_M/I_E) on the ambient temperature (Supporting Information, Figure S4). This allows an empirical curve of T versus I_M/I_E to be plotted with the known temperature from a thermostatic PS-Na solution bath (Figure 5c), which makes it possible to monitor the temperature evolution in the heating process (Figure 5d) with a sensitivity better than 1 °C. With 1.0 V voltage loading, 54 °C is reached from room temperature in 80 s following a linear relationship. The average heating rate is estimated to be $\approx 0.4\ ^\circ C\ s^{-1}$. The heating rate increases versus the voltage but a 5.0 V upper limit has been found for this circuit due to thermal damage. There is plenty of room to optimize the heating power by designing the circuit parameters, such as the wire thickness. This microheater set directly inside a microchannel may find great potential in further miniaturized MEMS, microsensors, and LoC systems for highly localized temperature regulation.

In conclusion, we have developed a flexible femtosecond-laser writing route for metal nanowiring on nonplanar substrates. Through careful control of laser power, the line width in the range of 125 to 500 nm could be easily adjusted. Any desired circuit or wire micropatterns could be directly written on various nonplanar substrates, such as a rough base, spherical surface, or even a sharp corner. Moreover, the patterned silver nanowires maintained a low resistivity of about $1.6 \times 10^{-7}\ \Omega m$, which imparts great potential for various circuitry and electronic interconnection uses. As a functional demonstration, a microheater inside a microchannel was successfully fabricated, which shows ideal heating capability towards microfluidic reactions. The femtosecond-laser-induced metal nanowiring could open a door to flexible integration of microcircuits, and renovate the route for the design and fabrication of integrated microcircuits in MEMS, LoC, and other intelligent microsystems.

Experimental Section

Preparation of silver precursor: The silver precursor was prepared by dripping a suitable amount of aqueous ammonia onto a mixture of silver nitrate aqueous solution ($0.083\ mol\ L^{-1}$) and trisodium citrate ($0.062\ mol\ L^{-1}$) under stirring until a clear solution was formed.

Preparation of microchannel: The microchannel was fabricated on a normal glass substrate by using photolithography and wet-etching techniques. Before usage, the chip was dipped in acetone and alcohol for 10 min each. Then it was further rinsed with distilled water and cleaned ultrasonically. Subsequently, the chip was dried with nitrogen gas.

Electrode coating: Au–Ge–Ni (Ge, 5%; Ni, 5%) strip films were deposited on the front side of the etched substrate by an evaporation technique. The thickness of the films was 200 nm and their resistivity was $6.2\ \Omega\ square^{-1}$.

Preparation of 3D polymeric microstructures: The frustums of pyramids and the hemisphere were made of SU-8 through TPA. The single-dot exposure time was 1000 μs. After femtosecond-laser writing, the resin SU-8 was post-baked at 95 °C for 10 min, and then developed in SU-8 developer for 60 min to remove the unsolidified liquid resin, thus leaving solid 3D microstructures on the substrate.

Femtosecond-laser processing: For each fabrication, the 790 nm femtosecond-laser pulse, with a width of 120 fs and mode locked at 82 MHz (from Tsunami, Spectra Physics), was tightly focused by a high-numerical-aperture (NA = 1.35) oil-immersion objective lens (100×). The laser power was controlled by a gradual neutral density filter. The focal spot was scanned laterally by steering a two-galvanomirror set while keeping along the optical axis by a piezo stage, both with high motion accuracy. The patterned silver structures were rinsed in distilled water for 10 min to remove the residual silver-ion solution. For heating tests, the chip was sealed by a film of PDMS at 200 °C under nitrogen gas.

The hemisphere and frustums of pyramids were fabricated by two-photon photopolymerization of the commercial resin SU-8, the refractive index of which is 1.56 at a wavelength of 532 nm. After femtosecond-laser direct writing according to preprogrammed microstructures, the resin SU-8 was post-baked at 95 °C for 15 min, and subsequently developed in SU-8 developer for 60 min to remove the unsolidified liquid resin and leave a solid skeleton.

Characterization: AFM images were obtained with a NanoWizard II BioAFM instrument (JPK Instruments AG, Berlin,

Germany). The absorption spectrum was obtained with a Shimadzu UV1700 spectrometer. SEM experiments were performed on a JEOL JSM-7500F scanning electron microscope (5.0 kV). Current–voltage curves of silver wires were measured with a Keithley SCS 4200 semiconductor characterization system. Optical micrographs were obtained from a Motic BA400 microscope and the charge-coupled device (CCD) of the laser.

Keywords:
electroless plating · interconnects · microheaters · nanowires · nonplanar substrates

[1] N. Maluf, K. Williams, *An Introduction to Microelectromechanical Systems Engineering*, Artech House, Boston **2004**.
[2] J. D. Plummer, M. D. Deal, P. B. Griffin, *Silicon VLSI Technology: Fundamentals, Practice and Modeling*, Prentice Hall, Upper Saddle River **2000**.
[3] F. Stellacci, C. A. Bauer, T. Meyer-Friedrichsen, W. Wenseleers, V. Alain, S. M. Kuebler, S. J. K. Pond, Y. Zhang, S. R. Marder, J. W. Perry, *Adv. Mater.* **2002**, *14*, 194.
[4] a) T. Tanaka, A. Ishikawa, *S. Kawata, Appl. Phys. Lett.* **2006**, *88*, 081107; b) A. Ishikawa, T. Tanaka, S. Kawata, *Appl. Phys. Lett.* **2006**, *89*, 113102; c) F. Formanek, N. Takeyasu, T. Tanaka, K. Chiyoda, A. Ishikawa, S. Kawata, *Appl. Phys. Lett.* **2006**, *88*, 083110.
[5] S. Maruo, T. Saeki, *Opt. Express* **2008**, *16*, 1174.
[6] A. I. Kuznetsov, A. B. Evlyukhin, C. Reinhardt, A. Seidel, R. Kiyan, W. Cheng, A. Ovsianikov, B. N. Chichkov, *J. Opt. Soc. Am. B* **2009**, *26*, B130.
[7] Y. Y. Cao, N. Takeyasu, T. Tanaka, X. M. Duan, S. Kawata, *Small* **2009**, *5*, 1144.
[8] B. H. Cumpston, S. P. Ananthavel, S. Barlow, D. L. Dyer, J. E. Ehrlich, L. L. Erskine, A. A. Heikal, S. M. Kuebler, I. Y. S. Lee, D. McCord-Maughon, J. Qin, H. Röckel, M. Rumi, X. L. Wu, S. R. Marder, J. W. Perry, *Nature* **1999**, *398*, 51.
[9] O. K. Kim, K. S. Lee, H. Y. Woo, K. S. Kim, G. S. He, J. Swiatkiewicz, P. N. Prasad, *Chem. Mater.* **2000**, *12*, 284.
[10] K. S. Lee, D. Y. Yang, S. H. Park, R. H. Kim, *Polym. Adv. Technol.* **2006**, *17*, 72.
[11] K. Sun, Z. Wang, X. Jiang, *Lab Chip* **2008**, *8*, 1536.
[12] J. Khandurina, T. E. McKnight, S. C. Jacobson, L. C. Waters, R. S. Foote, J. M. Ramsey, *Anal. Chem.* **2000**, *72*, 2995.
[13] K. Mølhave, B. A. Wacaser, D. H. Petersen, J. B. Wagner, L. Samuelson, P. Bøggild, *Small* **2008**, *4*, 1741.
[14] J. Yao, L. Zhong, Z. Zhang, T. He, Z. Jin, P. J. Wheeler, D. Natelson, J. M. Tour, *Small* **2009**, *5*, 2910.
[15] D. H. Kim, Z. Liu, Y. S. Kim, J. Wu, J. Song, H. S. Kim, Y. Huang, K-c. Hwang, Y. Zhang, J. A. Rogers, *Small* **2009**, *5*, 2841.
[16] N. Park, S. Kim, J. H. Hahn, *Anal. Chem.* **2003**, *75*, 6029.
[17] J. W. Jang, R. G. Sanedrin, A. J. Senesi, Z. Zheng, X. Chen, S. Hwang, L. Huang, C. A. Mirkin, *Small* **2009**, *5*, 1850.
[18] A. J. de Mello, M. Habgood, N. L. Lancaster, T. Welton, R. C. R. Wootton, *Lab Chip* **2004**, *4*, 417.
[19] Q. D. Chen, X. F. Lin, L. G. Niu, D. Wu, W. Q. Wang, H. B. Sun, *Opt. Lett.* **2008**, *33*, 2559.
[20] X. F. Lin, Q. D. Chen, L. G. Niu, T. Jiang, W. Q. Wang, H. B. Sun, *IEEE J. Lightwave Technol.* **2010**, *28*, 1256.
[21] Q. D. Chen, D. Wu, L. G. Niu, J. Wang, X. F. Lin, H. Xia, H. B. Sun, *Appl. Phys. Lett.* **2007**, *91*, 171105.
[22] J. Wang, H. Xia, B. B. Xu, L. G. Niu, D. Wu, Q. D. Chen, H. B. Sun, *Opt. Lett.* **2009**, *34*, 581.
[23] D. Wu, L. G. Niu, Q. D. Chen, R. Wang, H. B. Sun, *Opt. Lett.* **2008**, *33*, 2913.
[24] M. Maillard, P. Huang, L. Brus, *Nano Lett.* **2003**, *3*, 1611.
[25] B. Wiley, Y. Sun, B. Mayers, Y. Xia, *Chem. Eur. J.* **2005**, *11*, 454.
[26] S. A. Kalele, S. S. Ashtaputre, N. Y. Hebalkar, S. W. Gosavi, D. N. Deobagkar, D. D. Deobagkar, S. K. Kulkarni, *Chem. Phys. Lett.* **2005**, *404*, 136.
[27] Y. Sun, Y. Xia, *Science* **2002**, *298*, 2176.
[28] Y. Ding, F. Fan, Z. Tian, Z. L. Wang, *Small* **2009**, *5*, 2812.
[29] T. Tanaka, H. B. Sun, S. Kawata, *Appl. Phys. Lett.* **2002**, *80*, 312.
[30] H. Liang, Z. Li, W. Wang, Y. Wu, H. Xu, *Adv. Mater.* **2009**, *21*, 4614.
[31] H. Wang, N. J. Hala, *Adv. Mater.* **2008**, *20*, 820.
[32] Y. Sun, B. Mayers, T. Herricks, Y. Xia, *Nano Lett.* **2003**, *3*, 955.
[33] S. Juodkazis, N. Mukai, R. Wakaki, A. Yamaguchi, S. Matsuo, H. Misawa, *Nature* **2000**, *408*, 178.
[34] K. Sun, A. Yamaguchi, Y. Ishida, S. Matsuo, H. Misawa, *Sens. Actuators B* **2002**, *84*, 283.

Received: March 29, 2010
Published online: July 27, 2010